Large-area ultrathin Te films with substrate-tunable orientation

Elisabeth Bianco[*1†], *Rahul Rao*[2,3], *Michael Snure*[4], *Tyson Back*[2], *Nicholas R. Glavin*[2], *Michael E. McConney*[2], *P.M. Ajayan*[1,5], *Emilie Ringe*[*1,6,7].

[1]Department of Chemistry, Rice University, 6100 Main Street, Houston, TX 77005, United States

[2]Materials and Manufacturing Directorate, Air Force Research Laboratory, WPAFB, OH 45433, United States

[3]UES Inc., Dayton, OH 45432, United States

[4]Sensors Directorate, Air Force Research Laboratory, WPAFB, OH 45433, United States

[5]Department of Materials Science and NanoEngineering, Rice University, 6100 Main Street, Houston, TX 77005, United States

[6]Department of Materials Science & Metallurgy, University of Cambridge, 27 Charles Babbage Road, Cambridge, CB3 0FS, United Kingdom

[7]Department of Earth Sciences, University of Cambridge, Downing St, Cambridge, CB2 3EQ, United Kingdom

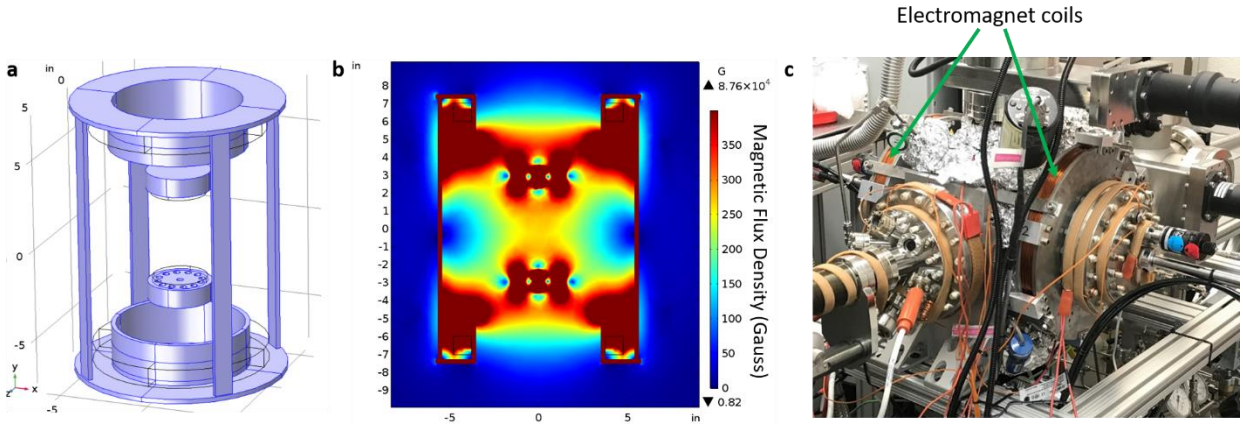

Figure S1. a) CAD drawing of the external electromagnet and magnetron geometries used in the finite element method (FEM) model in **b**. The outer confinement structure/flanges are soft Fe. b) 2D slice of the norm of the magnetic flux density in the sputtering chamber when equipped with 200-wire-turn electromagnets on either end (black boxes). FEM simulations were done in COMSOL. c) Photograph of the sputtering setup. External Helmholtz coils on either side of the deposition chamber are highlighted by green arrows.

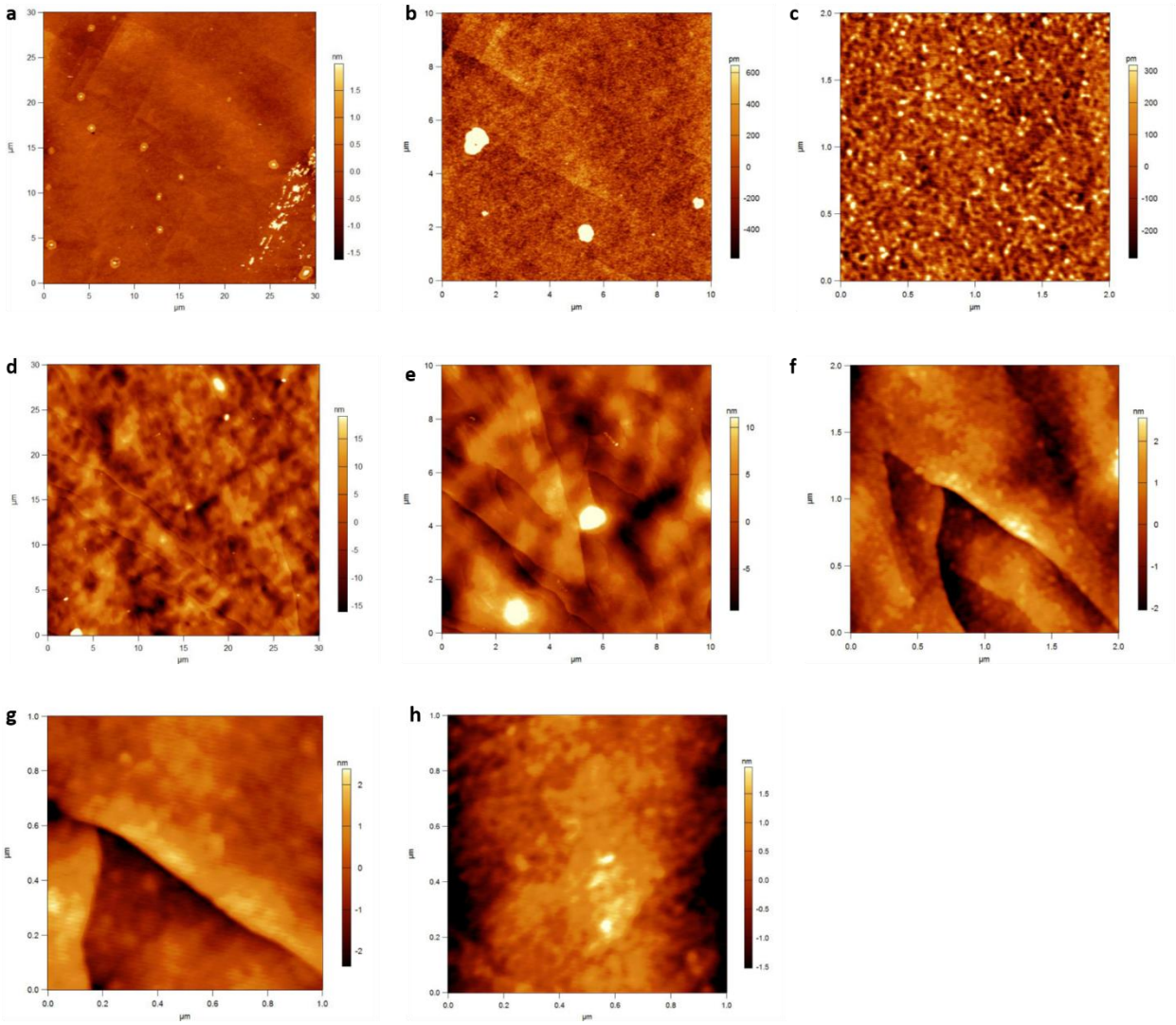

Figure S2. AFM topographical images at various fields of view of ultrathin Te grown on MgO (a-c) and HOPG (d-h).

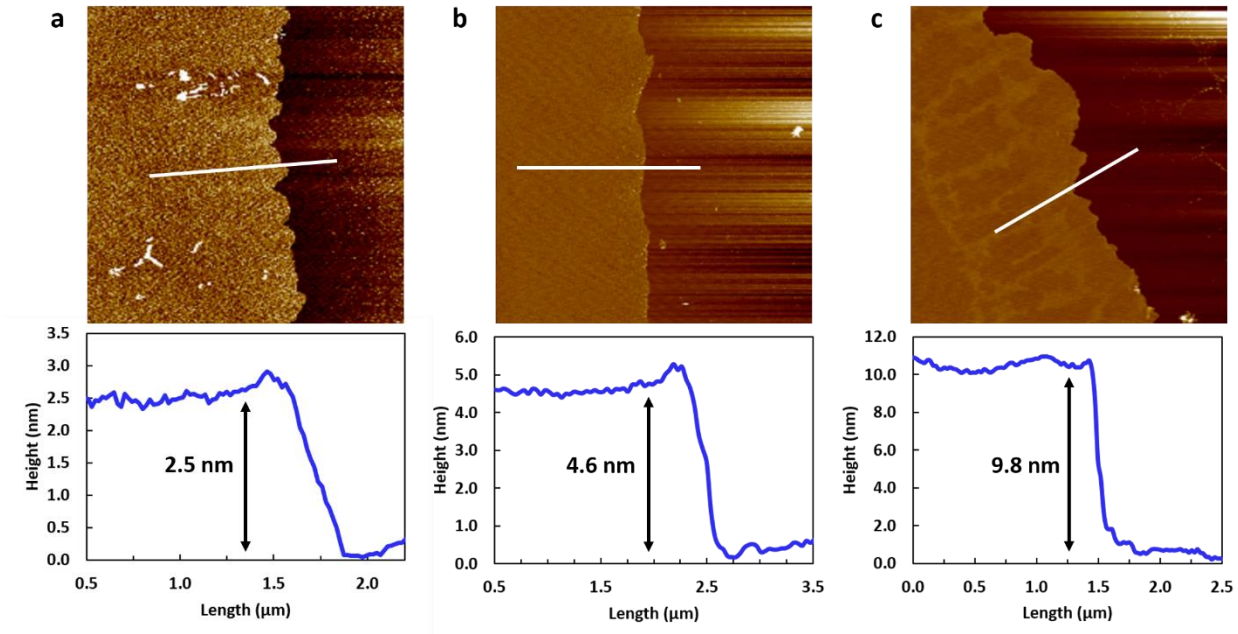

Figure S3. AFM images (top) and thickness profiles (bottom) of ulatrathin Te with thickness of a) 2.5 nm, b) 4.6 nm, and c) 9.8 nm.

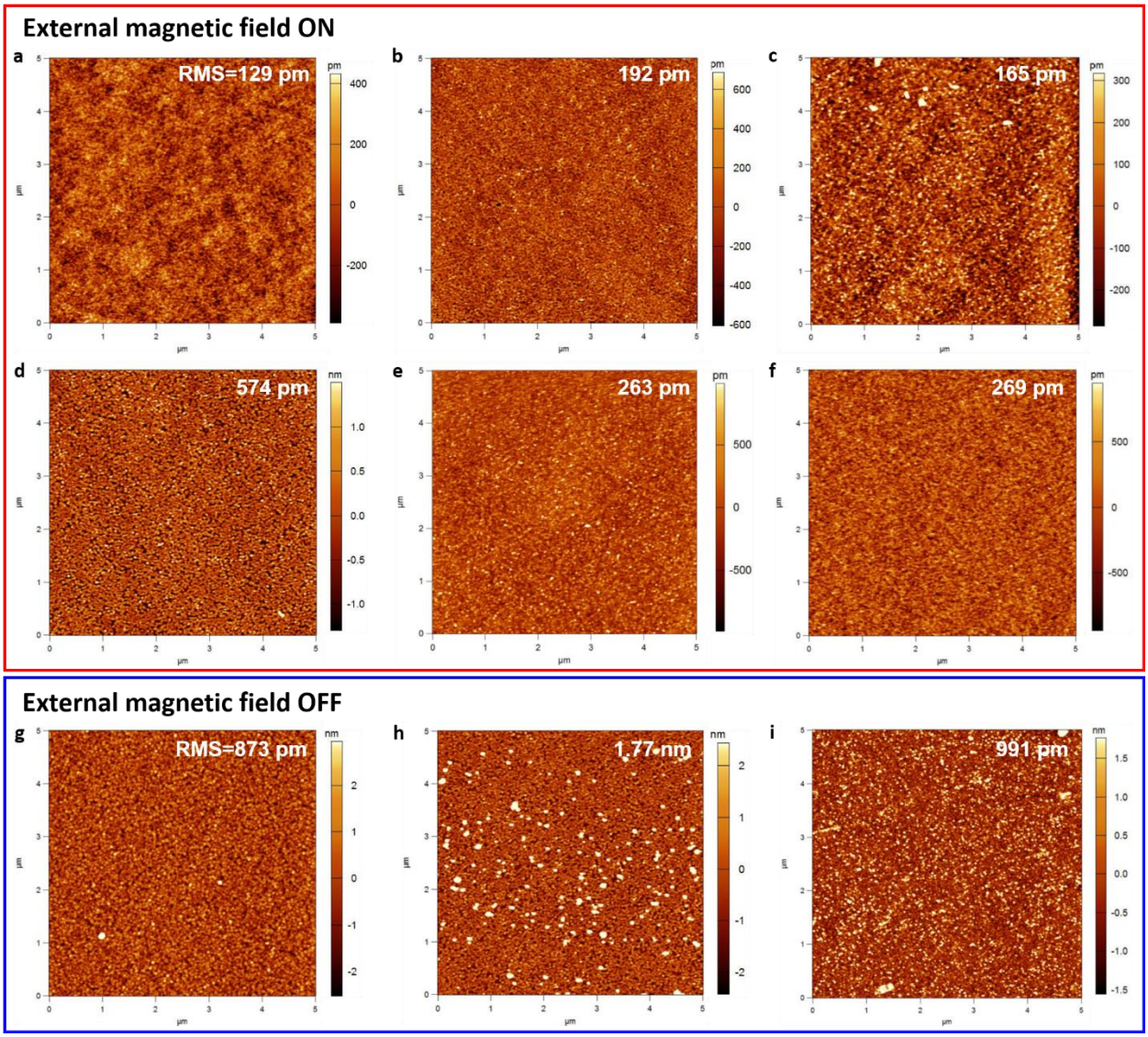
External magnetic field ON
a
RMS=129 pm
b
192 pm
c
165 pm
d
574 pm
e
263 pm
f
269 pm
External magnetic field OFF
g
RMS=873 pm
h
1.77 nm
i
991 pm

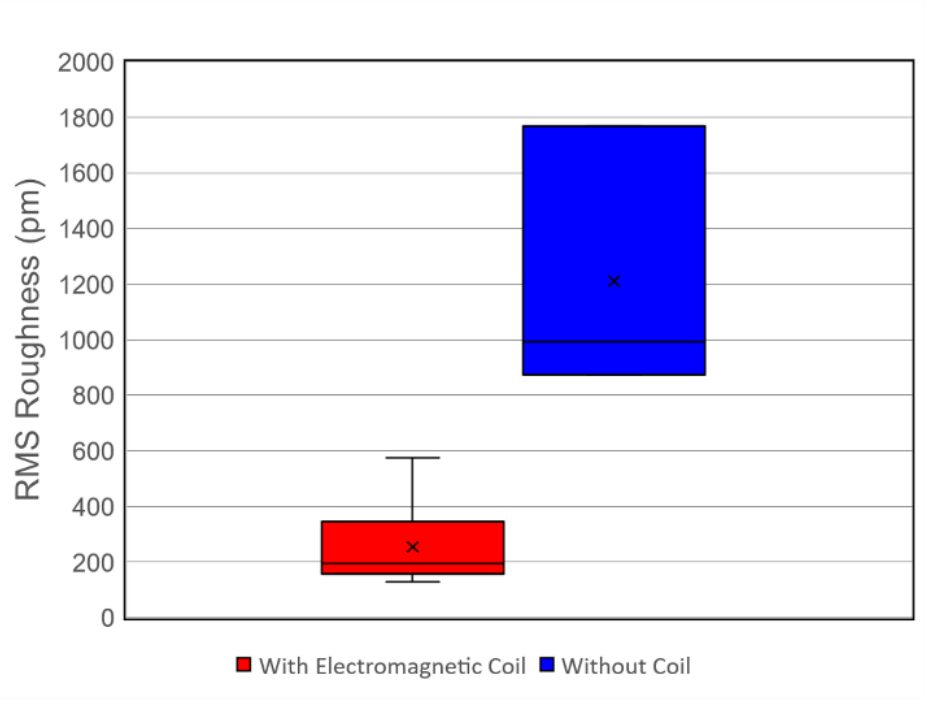

Figure S4. AFM topographical maps (top) from ultrathin Te grown with electromagnetic coils on (a-f) and electromagnetic coils off (g-i). Bottom) Statistical bar and whisker plot of images (a-g). Mean (x) and median (horizontal line) values are marked.

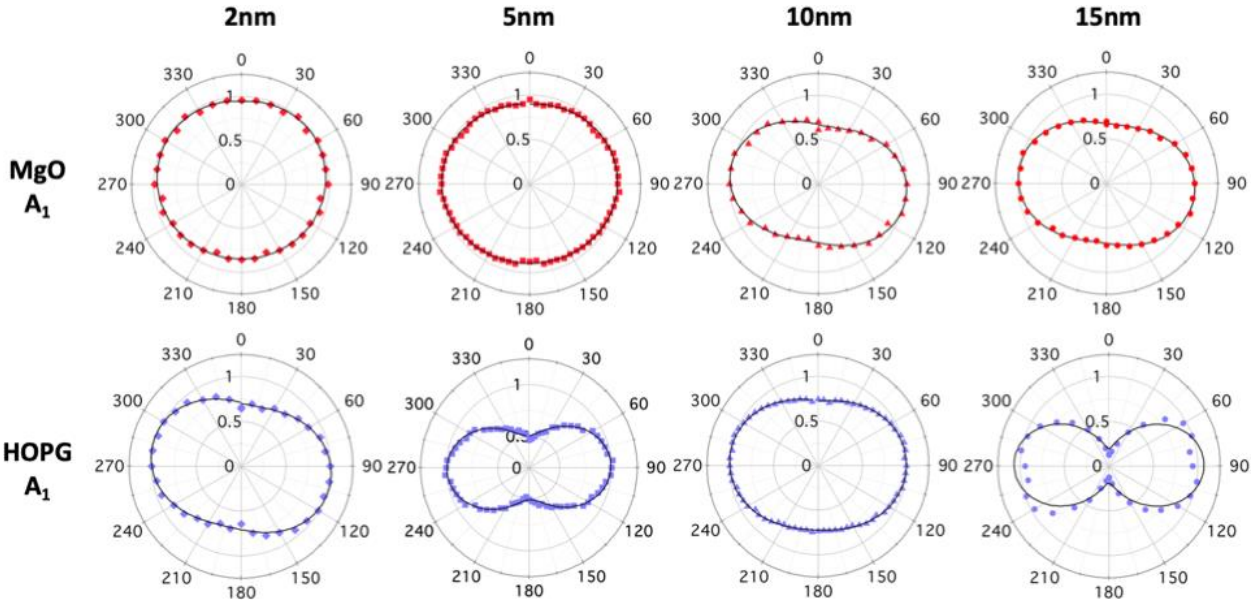

Figure S5. Radial Raman intensity profiles of the A_1 mode from MgO (top row) and HOPG (bottom row) for various Te film thicknesses.

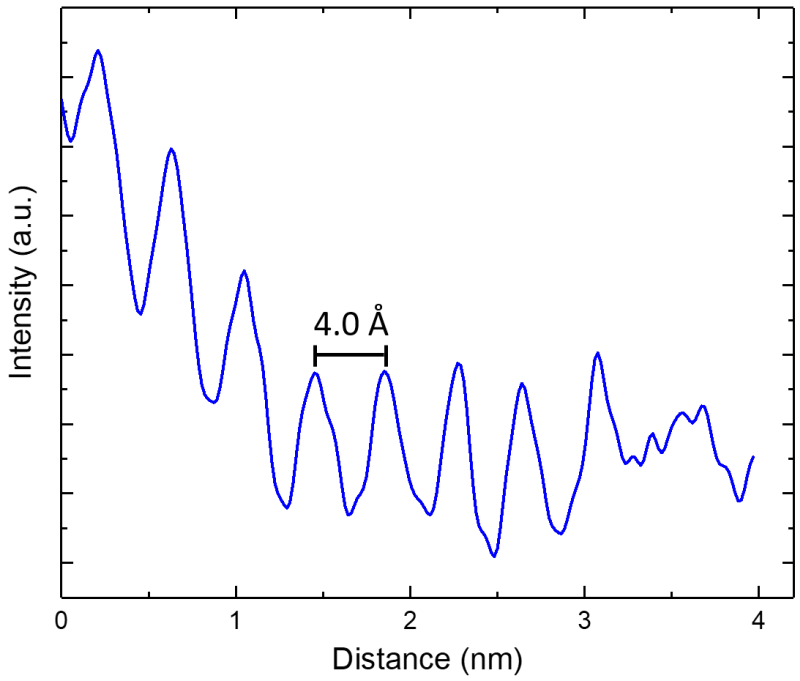

Figure S6. Line profile of the layer spacing of ultrathin Te from HRTEM in Figure 4.

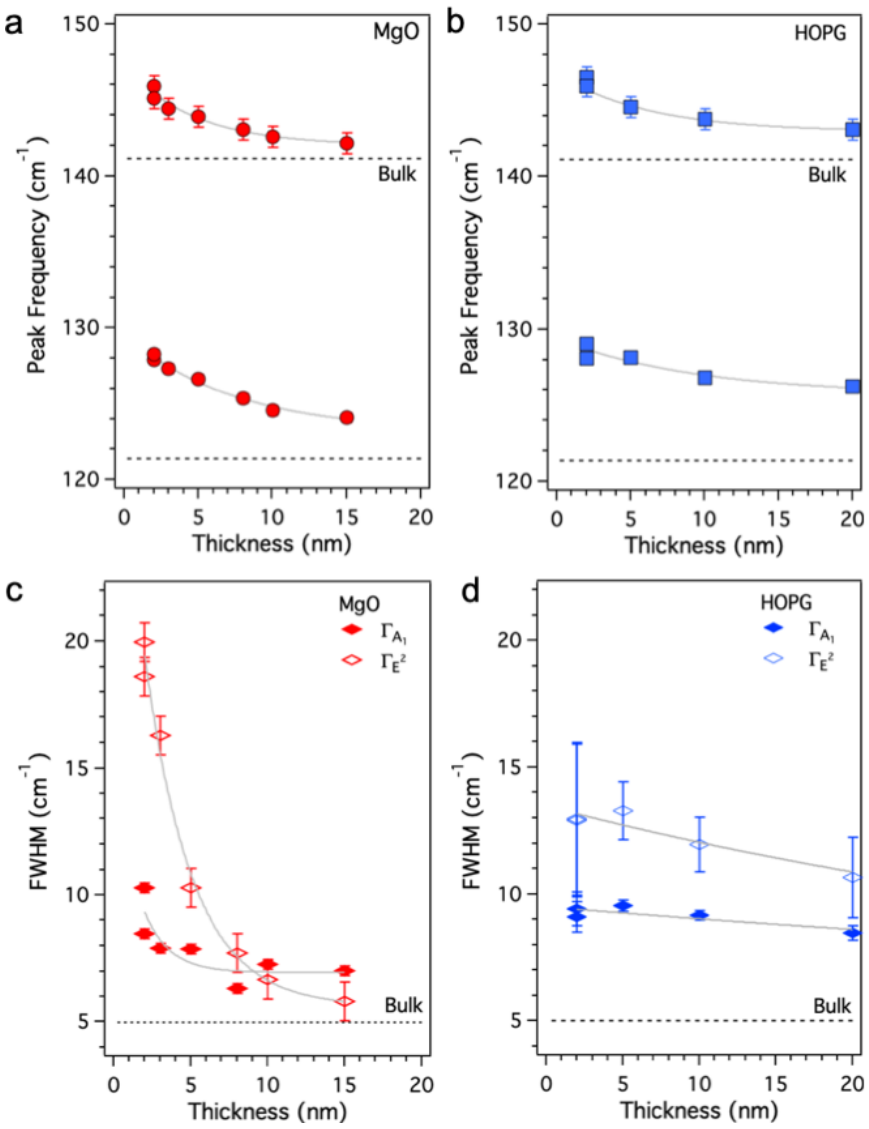

Figure S7. Raman peak frequencies as a function of film thickness from ultrathin Te films on (a) MgO and (b) HOPG. Peak linewidths (full width at half maximum intensity, FWHM) as a function of film thickness from Te films on (c) MgO and (d) HOPG.

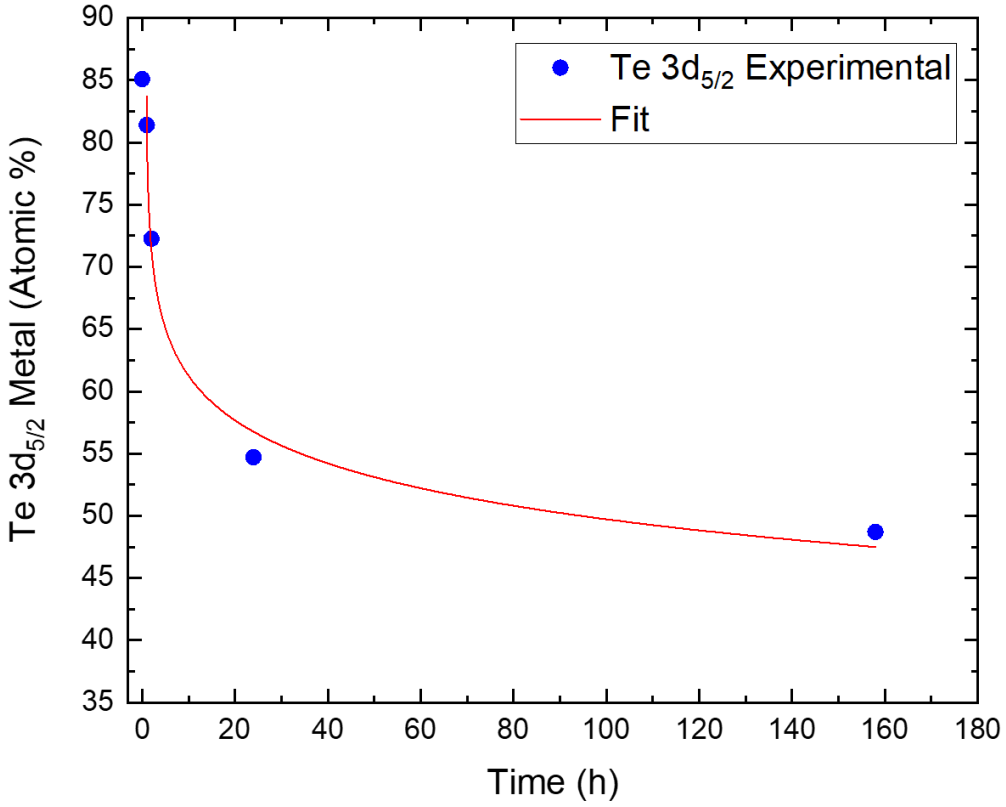

Equation	y = a – b*ln(x+c)
a	71.9 ± 3.0
b	4.84 ± 0.84
c	-0.86 ± 0.16
R-Square (COD)	0.990

Figure S8. XPS data of the change in atomic % of the Te^0 $3d_{5/2}$ metal peak (573.0 eV) as a function of time in ambient conditions. Experimental data (blue) was fitted to a logarithmic decay (red).